AD-A116 513 TUSKEGEE INST ALA SCHOOL OF ENGINEERING F/G 11/6
A STUDY OF CUMULATIVE FATIGUE DAMAGE IN 2011-T3 ALUMINUM ALLOY.(U)
AUG 81 S JEELANI, P A REDDY N00019-80-C-0564
UNCLASSIFIED TI-NAVY-3 NL

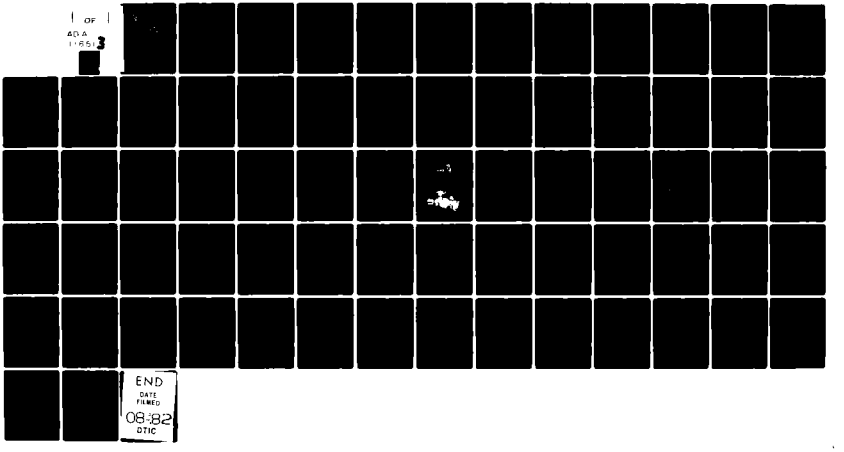

END
DATE FILMED
08-82
DTIC

(5)

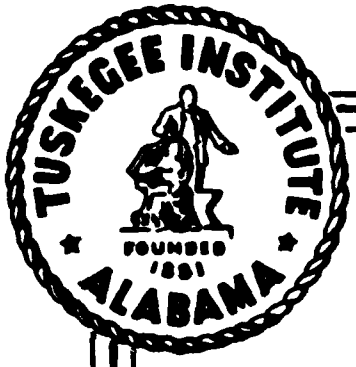

A STUDY OF CUMULATIVE FATIGUE DAMAGE IN 2011 - T3 ALUMINUM ALLOY

PURANDAR REDDY **SHAIK JEELANI**

Technical Report TI - NAVY - 3

AUGUST, 1981

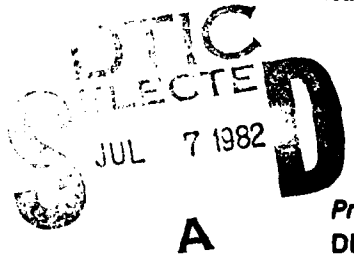

A

Prepared for:
DEPARTMENT OF NAVY
Naval Air Systems Command
Washington, D.C.
Contract N00019-80-C-0564

TUSKEGEE INSTITUTE
SCHOOL OF ENGINEERING
Tuskegee Institute, Alabama 36088

A STUDY OF CUMULATIVE FATIGUE DAMAGE IN 2011-T3 ALUMINUM ALLOY

Shaik Jeelani
Purander A. Reddy

Technical Report TI-NAVY-3 August 1981

Prepared For

DEPARTMENT OF THE NAVY
Naval Air Systems Command
Washington, D.C.

Contract No. N00019-80-C-0564

May 15, 1980-August 14, 1981

ABSTRACT

This report describes the experimental facility developed at Tuskegee Institute, Tuskegee, Alabama, to study the effect of cumulative fatigue damage in selected materials. The equipment procured consists of direct tension-compression fatigue testing machines Model DS-600 HLM and DS-6000 HLM instrumented to conduct fatigue tests on Aluminum, steel and super alloys under various stress sequences.

Specimen profiler, heat treatment furnace and electropolishing apparatus were purchased and/or developed for specimen preparation.

Experimental data were generated using 2011-T3 aluminum alloy specimens under stress ratios R=-1, R=-0.5, and R=0, for low-high, low-high mixed, and high-low mixed stress sequences.

Analysis of the data has indicated that the predicted cumulative fatigue damage and fatigue life are in close agreement for low-high and low-high mixed stress sequences under all stress ratios as compared with those obtained experimentally, whereas the theoretical values for high-low and high-low mixed stress sequences under all stress ratios were more conservative than those obtained experimentally.

A

TABLE OF CONTENTS

LIST OF FIGURES

LIST OF TABLES

TABLES (Continued)

INTRODUCTION

The performance of structural and machine parts under dynamic loads is frequently associated with repeated stress cycles of high amplitudes varying over a wide range. This particularly applies to parts of aircrafts, ships, railway engines and coaches, motor vehicles, bridges, and transmission cables, etc.

Repeated loads are a major cause for the reduction in allowable stresses, below those listed for various static properties such as yield strength, ultimate strength, etc. In those loadings the sequence of varying load magnitudes occurs more or less in a random manner.

The prediction of fatigue concerns with the estimation of the time length that a material can serve the intended design functions when subjected to varying stress conditions. Due to the various possible stress patterns, it does not appear that fatigue life results can be compiled for complex stress patterns similar to that accumulated for pure sinosoidal stress histories. This gives an indication that for complex stress histories a certain amount of analysis must be resorted to in order to overcome the expected deficiency in test data directly relating to particular histories.

In laboratories it is a standard practice to test the specimens at constant load amplitudes and obtain a S-N curve. In the actual situations the load of each part critical in fatigue varies a great

deal. To design the part which resists the service load using the S-N curve an equation was proposed by Palmgren and was later reproposed by Miner (1). These are various other methods proposed, such as Grover's theory (2), Marco Starkey's theory (3), Shanley's theory (4), Corten Dolan's theory (5), Freudenthal-Heller theory (6), etc., but none of these can be relied on to predict fatigue life with any accuracy for most of the commonly encountered circumstances. The Miners theory which is most commonly used in majority of the applications does not depend on the previous history of the material or its behavior in multi-level loading.

Based on these and other researchers' experimental and theoretical investigations and his own, Kramer (7,8) concluded that when subjected to stress-cyclic process, the work hardening of metal is confined to primarily the surface layer. With the increase in number of cycles and the stress amplitudes there is an increase in the surface layer stress. As the fatigue damage accumulates the surface layer stress reaches a critical value and a fatigue propagation crack is formed independent of the stress amplitude leading to fatigue failure. He proposed that cumulative fatigue damage and cumulative fatigue life can be described in terms of rate of increase in the strength of the surface layer with the number of cycles. Since the critical surface stress is constant for a particular metal it is only needed to determine the contribution to the surface stress by cycling at an applied stress for a given number of cycles and sum up the contributions until

failure occurs.

Analyzing this argument, Kramer developed an equation for predicting cumulative fatigue damage, which is

$$\left[{}_{1}P_{N_1} + {}_{2}P_{N_2}\left(\frac{\quad}{\quad}\right)^{Pf_1} + {}_{3}P_{N_3}\left(\frac{\quad}{\quad}\right)^{Pf_2}\left(\frac{\quad}{\quad}\right)^{Pf_2 f_1} + \ldots \right] = \frac{S^*}{\quad} = \quad \tag{1}$$

where $f_1 = {}_{1}P_{N_1}$, $f_2 = {}_{2}P_{N_2}\left(\frac{\quad}{\quad}\right)^{Pf_1}$ and so on are the damage histories in the previous stages of the stress-cycles loading process.

The equation can also be expressed as

$$\left[\frac{P_{N_1}}{\quad} + \frac{P_{N_2}}{\quad}\left(\frac{\quad}{\quad}\right)^{Pf_1} + \frac{P_{N_3}}{\quad}\left(\frac{\quad}{\quad}\right)^{Pf_2}\left(\frac{\quad}{\quad}\right)^{Pf_2 f_1} + \ldots \right] = 1 \tag{2}$$

which means that when the cumulative fatigue damage for all the stages equals one failure will occur.

A detailed development of the equation is shown in Appendix D.

CHAPTER I

INSTALLATION AND CALIBRATION OF FATIGUE MACHINE

The direct stress fatigue machines DS-600 and DS-6000 HLM are designed for testing in tension and/or compression up to 600 and 6000 pounds of total load, respectively. Each machine, as shown in Figure 1, is equipped with a power base consisting of a one horse power variable speed drive motor, a control cabinet, a cycle counter, and a variable eccentric crank and connecting rod. The dynamic loading system includes a load frame and the load lever. One end of the load lever is pivoted in a parallelogram flexture assembly which creates a straight line loading at the load stud and the other end is attached to the variable eccentric crank.

Mounted on the load frame are the hydraulic load maintainer system and hydraulic cylinder. The upper load stud is attached to the hydraulic cylinder. The load maintainer system includes load sensing contact units mounted on the base on either side of the load lever and a solid state electronic control system in the control cabinet. The pumping unit consists of two continuously running piston pumps immersed in oil and driven by an eccentric on a single phase constant speed motor. Each pump has a relief, check, and back pressure valve controlled by a solenoid which is activated by the load sensing units. These contact units will prevent the maximum load

from decreasing. When the load on the specimen increases or decreases, the load lever will make contact with the sensing unit which will activate the proper solenoid. The solenoid will activate the pump and send more pressure to the side of the hydraulic piston as required to increase or decrease the load. The load sensing units will also stop the machine if the specimen fails or the hydraulic maintainer cannot keep the load from dropping rapidly.

A fatigue rated strain gage load transducer fitted to the upper load stud is used to read the load. The transducer can remain on the machine while the machine is in use. The leads from the transducer are connected to a strain indicator which is calibrated for reading the load directly in pounds.

For calibrating the strain indicator, the loading lever is disconnected from the variable eccentric crank. A load of 25 pounds is applied at the free end of the loading arm and the strain indicator is adjusted to read the load directly. Additional loads of 50 and 75 pounds, respectively, are applied to check the calibration.

Once calibrated, the machine is capable of performing five different types of loading: "zero to tension," "zero to compression," "tension to tension," "compression to compression," and "tension to compression."

The cyclic load is applied by changing the throw on the variable eccentric from zero throw through the rotation of the eccentric using the manually wrenched pinnion drive. This change in the throw of the

eccentric will cause deflection of the load lever and the deflection will be transmitted as load to the specimen through the flexure system. For any given test set up the eccentric crank setting will create the same cyclic load regardless of the mean load.

After the cyclic load is established, depending upon the testing condition required, the mean load can be adjusted to the desired value using the UP and DOWN switches on the control cabinet. These switches also regulate the hydraulic load maintainer. Once the cyclic load and mean load are established, the machine is ready for testing.

CHAPTER II

SPECIMEN PREPARATION

The fatigue specimen designed for the investigation is shown in Figure 2. The threaded ends of the specimen were made long enough to accommodate locknuts to avoid slackening at the grips. The grips for holding the specimens were custom designed. The length to diameter ratio of the gauge section of the specimen was chosen as 2:1 to avoid buckling during compression.

After carefully machining the specimen, as per the design specifications, the gauge section was prepolished with grade 600 and 800 silicon carbide papers to reduce the tool marks and other surface irregularities. This was followed by electropolishing to obtain an even surface finish.

The electropolishing device designed for polishing the specimen is shown in Figures 3, 4, and 5. The specimen itself is the anode and is rotated by a motor at a predetermined speed. The cathode consists of a 25-gauge stainless steel sheet bent cylindrically to maintain uniform distance between the anode and cathode. The stainless steel sheet is placed in a glass container filled with electrolyte which is a mixture of methanol, butyl cellosolve, and perchloric acid. A magnetic stirrer was used to stir the electrolyte to maintain uniform strength throughout the electrolyte. The glass container was

immersed in an ice bath to maintain the temperature of the electrolyte at 15°C. A detailed procedure for electropolishing the specimen is shown in Appendix E.

CHAPTER III

EXPERIMENTAL PROCEDURE

After electropolishing, the specimen was carefully examined under a microscope for circumferential tool marks and stress risers. The specimen was then placed in the machine grips by positioning the upper load screw by means of the nuts on either side of the piston. Then, by changing the variable eccentric crank the required load range was obtained. Then based on the stress ratio condition for the test, the mean load was set. The testing for each specimen was done in four different stages. For the first stage through the third stage the load set and the number of cycles applied at that particular load was predetermined. In the last (fourth) stage after setting the load the test was allowed to continue until the specimen failed. Under each of the three different stress ratios, i.e., R=-1, R=-0.5, and R=0, tests were conducted with four different stress sequences: (i) high to low stress sequence, (ii) high to low mixed sequence, (iii) low to high stress sequence, and (iv) low to high mixed stress sequence.

Figure 9 (Appendix A) shows the stress cycling to obtain various values of R.

CHAPTER IV

ANALYSIS OF DATA

To calculate the slope and the intercept on the vertical axis, a statistical method was used with the S-N curve line equation being log = m.(logN) + logC.

	X--log N	Y--log	XY	X^2
1	3.61278	4.62557	16.71117	13.05215
2	3.90309	4.56591	17.82116	15.23411
3	4.05690	4.53865	18.28132	16.45844
4	4.31175	4.50623	19.42974	18.59119
5	4.63144	4.46015	20.65692	21.45020
6	4.86094	4.42911	21.52964	23.62874
7	4.91169	4.37791	21.50294	24.12470
8	5.16732	4.34502	22.45211	26.70120
9	5.48855	4.28212	23.50263	30.12418
n = 9	εX = 40.94446	εY = 40.13067	εXY = 181.88763	εX^2 = 189.36494

$$\text{Therefore, slope } (m) = \frac{n.\varepsilon XY - \varepsilon X.\varepsilon Y}{n.\varepsilon X^2 - (\varepsilon X)^2}$$

$$= \frac{(9)\ (181.88763) - (40.94446)\ (40.13067)}{(9)\qquad (189.36494) - (40.94446)^2}$$

$$= -0.2206$$

$$\text{and intercept } (\log C) = \frac{\varepsilon Y.\varepsilon X^2 - \varepsilon X.\varepsilon XY}{n.\varepsilon X^2 - (\varepsilon X)^2}$$

$$= \frac{(40.13067)\ (189.36494) - (40.94446)\ (181.88763)}{(9)\qquad (189.36494) - (40.94446)^2}$$

$$= 5.4625$$

Calculation of material constants p and

$$p = -\frac{1}{M} = -\frac{1}{-0.2206} = 4.533$$

and $C = (\log^{-1} C)^p = (\log^{-1} 5.4625)^{4.533} = 5.7745 \times 10^{24}$

Calculation of fatigue damage using Kramer's equation under completely reversed stress conditions where in the first three stages of the testing the following maximum stress number of cycles were used:

$\sigma_1 = 25000$ Psi, $N_1 = 20000$ cycles

$\sigma_2 = 30000$ Psi, $N_2 = 8000$ cycles

$\sigma_3 = 35000$ Psi, $N_3 = 4000$ cycles.

In the final stage, maximum stress of 40000 Psi was applied and the test was allowed to run until the specimen failed. The specimen failed after 2400 cycles (the calculations shown here are for specimen 2 in the low to high stress sequence).

Damage in the first stage $= f_1 = \frac{N_1 \sigma_1^P}{C} = \frac{(20000)\ (25116)^{4.533}}{(5.7745)\ (10)^{24}}$

$= 0.305$

Damage in the second stage $= f_2 = \frac{N_1 \sigma_1^P}{C}\left(\frac{\sigma_1}{\sigma_2}\right)^{Pf_1}$

$= \frac{(8000)\ (30090)^{4.533}}{(5.7745)\ (10)^{24}} \left(\frac{25116}{30090}\right)^{(4.533)\ (0.305)}$

$= 0.216$

Damage in the third stage $= f_3 = \frac{N_3 \sigma_3^P}{C}\left(\frac{\sigma_2}{\sigma_3}\right)^{Pf_2} \left(\frac{\sigma_1}{\sigma_2}\right)^{Pf_2 f_1} =$

$\frac{4000 \times (35063)^{4.533}}{5.7743 \times 10^{24}} \left(\frac{30090}{35063}\right)^{4.533 \times 0.216} \left(\frac{35116}{30090}\right)^{4.533 \times 0.216 \times 0.305} =$

0.226.

Damage in the fourth stage = $f_4 = \frac{N_4 \sigma_4^P}{\beta}\left(\frac{\sigma_3}{\sigma_4}\right)^{Pf_3}\left(\frac{\sigma_2}{\sigma_3}\right)^{Pf_3f_2}\left(\frac{\sigma_1}{\sigma_2}\right)^{Pf_3f_2f_1}$

$= \frac{2400 \times (39789)^{4.533}}{5.7745 \times 10^{-24}} \left(\frac{35063}{39789}\right)^{1.024} \times \left(\frac{30090}{35063}\right)^{0.221} \times \left(\frac{25116}{30090}\right)^{0.067} = 0.247.$

Therefore, cumulative fatigue damage $D_F = f_1 + f_2 + f_3 + f_4$

$= 0.305 + 0.216 + 0.226 + 0.247$

$= 0.994.$

Prediction of Fatigue Life:

The following calculation shows the prediction of the number of cycles required to cause failure in the last (fourth) stage:

$f_4 = D_F - (f_1 + f_2 + f_3) = 1 - (0.305 + 0.216 + 0.226)$

$= 1 - 747 = 0.253.$

$f_4 = \frac{N_4 \sigma_4^P}{\beta}\left(\frac{\sigma_3}{\sigma_4}\right)^{Pf_3}\left(\frac{\sigma_2}{\sigma_3}\right)^{Pf_3f_2}\left(\frac{\sigma_1}{\sigma_2}\right)^{Pf_3f_2f_1}$

$0.253 = N_4 (1.0303 \times 10^{-4})$

No. of cycles to failure N_4 = 2456 cycles.

CHAPTER V

DISCUSSION OF RESULTS

The fatigue strength versus fatigue life (S-N) curves plotted for the stress ratios of -1, -0.5, and 0, using the test data shown in Tables 1, 2, and 3, are shown in Figure 6. A statistical method was used as shown in the analysis to determine the slopes of the curves. The constant life diagram shown in Figure 7 was obtained using the S-N curves.

Tables 4-7 show the cumulative fatigue data for the completely reversed stress conditions, R=-1. Table 4 shows the data for the low-high stress sequence. For the specimens 1-6 the stress in the first stage was 25 Ksi for 20000 cycles, 30 Ksi in the second stage for 8000 cycles, 35 Ksi for 4000 cycles in the third, and stressed until failure of the specimens at 40 Ksi. For specimens 7-9 the stress sequence was 25 Ksi for 30000 cycles, 30 Ksi for 10000 cycles, 35 Ksi for 3000 cycles, and 40 Ksi until failure took place. For specimens 10-12, the stress pattern was 25 Ksi for 25000 cycles, 30 Ksi for 10000 cycles, 35 Ksi for 5000 cycles, and finally in the last stage 40 Ksi until failure took place.

For specimens 13-15, the low to high stress sequence was 20 Ksi for 35000 cycles, 25 Ksi for 30000 cycles, 30 Ksi for 15000 cycles, and stressed at 35 Ksi in the last stage until the specimens failed.

In the low-high stress pattern, for all the specimens, it was observed that there was a close agreement between the experimental and theoretical fatigue life values in the final (fourth) stage.

Table 5 shows the data for the low-high mixed stress sequence. For the specimens 1-6 the stress applied was 25 Ksi for 20000 cycles, increased to 35 Ksi for 4000 cycles, reduced to 30 Ksi for 8000 cycles, and finally stressed at 40 Ksi until failure took place.

Similarly for specimens 7-9, it was 25 Ksi for 30000 cycles, 35 Ksi for 3000 cycles, 30 Ksi for 10000 cycles, and 40 Ksi until the specimen failed. For specimens 10-12, it was 25 Ksi for 25000 cycles, 35 Ksi for 5000 cycles, 30 Ksi for 11000 cycles, and 40 Ksi until failure took place.

For specimens 13-15, the stress pattern was 20 Ksi for 35000 cycles, 30 Ksi for 15000 cycles, 25 Ksi for 25000 cycles, and stressed at 35 Ksi in the fourth stage until failure took place. The specimens 16-18 were subjected to a stress sequence of 20 Ksi for 40000 cycles, 30 Ksi for 16000 cycles, 25 Ksi for 20000 cycles, and 35 Ksi in the last stage until failure took place.

For the low-high mixed stress sequence it was observed that there was a close agreement between the experimental and theoretical values of fatigue life in the fourth stage.

Table 6 shows the data for the high-low stress sequence. For specimens 1-6 a stress of 40 Ksi was applied for 1500 cycles in the first stage. Then the stress was decreased to 35 Ksi for 4000 cycles,

and in the third stage it was further reduced to 30 Ksi for 8000 cycles. In the last stage the specimens were stressed until failure at 25 Ksi. For specimens 7-9 the stress sequence was 40 Ksi for 2500 cycles, 35 Ksi for 6000 cycles, 30 Ksi for 15000 cycles, and finally 25 Ksi until failure took place. For specimens 10-12, the stress sequence was 40 Ksi for 3000 cycles, 35 Ksi for 5000 cycles, 30 Ksi for 20000 cycles, and 25 Ksi until failure took place.

For specimens 13-15, in the first stage of testing a stress of 35 Ksi was applied for 5000 cycles. In the second stage it was 30 Ksi for 12000 cycles, the third stage 25 Ksi for 25000 cycles, and in the last stage at 20 Ksi they were stressed until failure. Likewise, for specimens 16-18 the sequencing was 35 Ksi for 4000 cycles, 30 Ksi for 15000 cycles, 25 Ksi for 30000 cycles, and in the last stage 20 Ksi and were stressed until failure.

For all the specimens it was observed that by testing at a high stress initially and then gradually reducing the stress in each stage, there was an increase in the fatigue life. It was also observed that the fatigue life, when stressed at 25 Ksi after initially stressing at 40 Ksi, 35 Ksi, and 30 Ksi, was about six times higher than the theoretical life at that stress.

Table 7 shows the data for the high-low mixed stress sequence. In the high-low mixed stress sequence the specimens 1-6 were subjected to a stress of 40 Ksi for 1500 cycles in the first stage. In the second stage the stress was reduced to 30 Ksi for 8000 cycles and in the third stage the stress was increased to 35 Ksi for 4000 cycles before finally

applying a stress of 25 Ksi where the specimens were stressed until failure took place.

For specimens 7-9 the stress sequencing was 40 Ksi for 3500 cycles, 30 Ksi for 9000 cycles, 35 Ksi for 5000 cycles, and 25 Ksi until failure of the specimens took place. For specimens 10-12 it was 40 Ksi for 3000 cycles, 30 Ksi for 11000 cycles, 35 Ksi for 7000 cycles, and in the last stage 25 Ksi until failure took place.

For specimens 13-15 a different high-low mixed stress sequence was used. In the first stage the maximum stress was 35 Ksi for 5000 cycles and in the second stage it was decreased to 25 Ksi for 15000 cycles. In the third stage the stress was increased to 30 Ksi for 30000 cycles, and in the last stage the stress was reduced to 20 Ksi and the specimens were stressed until failure took place.

Again, for all the specimens tested under high-low mixed stressed sequence it was observed that the fatigue life values obtained experimentally were much higher than those obtained theoretically.

From the Tables 6 and 7 it can be seen that theoretically for all the specimens 7-18 for the high-low stress sequence and specimens 7-18 for the high-low mixed stress sequence failure should have occurred in the third stage itself.

Tables 16-19 show the cumulative fatigue damage and the total number of cycles obtained theoretically using the Kramer equation and also experimentally. From that, it can be observed that for the low-high and low-high mixed stress sequences the predicted fatigue life and the experimental fatigue life are in complete agreement, whereas

for the high-low and high-low mixed stress sequences the predicted fatigue life is very conservative when compared to the experimental values.

Tables 8-11 show the data for the cumulative fatigue for the stress ration of R=-0.5. Table 8 shows the data for high-low stress sequence. In this sequence, for specimens 1 and 2 the maximum stress applied was 40 Ksi for 4000 cycles in the first stage. In the second stage stress was 35 Ksi for 8000 cycles, and in the third stage it was 30 Ksi for 30000 cycles. In the fourth stage the specimens were stressed until failure at 25 Ksi. For specimens 3 and 4, the stress sequence was 40 Ksi for 5000 cycles, 35 Ksi for 7000 cycles, 30 Ksi for 35000 cycles, and stressed until failure occurred at 25 Ksi.

Table 9 shows the data for high-low mixed stress sequence. For specimens 1 and 2, the sequence was 40 Ksi for 4000 cycles, 30 Ksi for 30000 cycles, 35 Ksi for 8000 cycles, and 25 Ksi until the specifailed. For specimens 3 and 4, the stress sequencing was 40 Ksi for 5000 cycles, 30 Ksi for 35000 cycles, 35 Ksi for 7000 cycles, and in the last stage stressed at 25 Ksi until failure occurred.

In both the high-low and high-low mixed stress sequences it was observed that the fatigue life in the last stage was much higher experimentally than that obtained theoretically. For specimens 3 and 4, in both the high-low and high-low mixed stress sequences theoretically failure should have occurred in the third stage, whereas the specimens failed eventually in the fourth stage.

Table 10 shows the data for low-high stress sequence in which for specimens 1-3 it was 25 Ksi for 60000 cycles in the first stage, 30 Ksi in the second for 30000 cycles, 35 Ksi for 800 cycles in the third, and finally stressed until failure took place at 40 Ksi. In the case of the specimens 2 and 3, the stress sequence was 25 Ksi for 50000 cycles, 30 Ksi for 25000 cycles, in the second stage, and 35 Ksi in the third stage. Even though the specimens were not stressed until failure occurred, the specimens failed before reaching 1/3 of the theoretical fatigue life at that particular stress. Similar observation was made for specimens 2 and 3. For specimen 1, the predicted life was about 2 to 3 times more than the experimental value.

Table 11 shows the data for low-high mixed stress sequence where the specimens 1-3 were subjected to a stress of 25 Ksi for 6000 cycles in the first stage, and 35 Ksi for 8000 cycles in the second stage. In the third stage the specimens were subjected to a stress of 30 Ksi and even though they were not stressed until failure, the specimens failed. For the specimens 4 and 5, the same pattern was observed where in the first stage the stress was 25 Ksi for 50000 cycles and in the second stage 35 Ksi for 9000 cycles. The specimens failed in the third stage when subjected to a stress of 30 Ksi. For all the specimens tested under the low-high mixed stress sequence, the theoretical fatigue life at 30 Ksi after being subjected to stresses of 25 Ksi and 35 Ksi in the previous stages was nearly twice as much as that obtained experimentally.

Tables 20-23 show the cumulative fatigue damage using Kramer's equation and the Miners equation. They also show the fatigue life

values obtained theoretically as well as experimentally. The theoretical fatigue life values for the high-low and the high-low mixed stress sequences were observed to be very conservative. The values of the fatigue life for the low-high and the low-high mixed stress sequences, theoretically, were considerably closer to those obtained experimentally.

Tables 12-15 show the data for cumulative fatigue for the stress ratio R=0. Table 12 shows the data for high-low stress sequence where specimens 1 and 2 were subjected to 40 Ksi for 12000 cycles in the first stage, 35 Ksi for 25000 cycles in the second stage, 30 Ksi for 50000 cycles in the third stage, and finally stressed until failure at 25 Ksi. Specimens 3 and 4 were subjected to stresses of 40 Ksi for 20000 cycles, 35 Ksi for 30000 cycles, 30 Ksi for 40000 cycles, and 25 Ksi until the specimens failed.

For specimens 1 and 2, it was observed that the experimental fatigue life at 25 Ksi (final stage) was about twice the value obtained theoretically. As for specimens 3 and 4, it was observed that the experimental fatigue life at 25 Ksi was about six times higher than the theoretical value at the same stress.

Table 13 shows the data for high-low mixed stress sequence. Specimens 1 and 2 were stressed at 40 Ksi for 20000 cycles, 30 Ksi for 50000 cycles, 35 Ksi for 25000 cycles, and finally in the last stage 25 Ksi until failure occurred. For specimens 3 and 4, the stress was 40 Ksi for 25000 cycles, 30 Ksi for 40000 cycles, 35 Ksi for 20000 cycles, and 25 Ksi until failure occurred. For all the specimens, it was

observed that the experimental fatigue life values at 25 Ksi were about seven times higher than the theoretical values.

Table 14 shows the data for the low-high stress sequence. Specimens 1 and 2 were subjected to 25 Ksi for 150000 cycles, 30 Ksi for 40000 cycles, 35 Ksi for 20000 cycles, and in the last stage stressed at 40 Ksi until failure took place. The specimens 3 and 4 were stressed at 25 Ksi for 200000 cycles, 30 Ksi for 45000 cycles, 35 Ksi for 15000 cycles, and 40 Ksi until the specimens failed. The experimental fatigue life values for the specimens tested under the low-high stress sequence at 40 Ksi were about one and one-half times higher than those obtained theoretically at the same stress.

Table 15 shows the data for low-high mixed stress sequence. For specimens 1 and 2, the stress sequence was 25 Ksi for 200000 cycles, 35 Ksi for 25000 cycles, 30 Ksi for 45000 cycles, and 40 Ksi until failure took place. The stress sequence for specimens 3 and 4 was 25 Ksi for 150000 cycles, 35 Ksi for 20000 cycles, 30 Ksi for 40000 cycles, and in the final stage 40 Ksi until the specimens failed. The same pattern was observed in the fatigue life values in the last stage as those for the low-high stress sequence. The experimental values were about one and one-half times higher than the theoretical values.

Tables 24-27 show the cumulative fatigue damage using Kramer's equation and Miner's equation. They also show the predicted and experimental fatigue life values. Again, the same observation was made

as for the values for R=-1 and R=-0.5. The values obtained theoretically for high-low and high-low mixed stress sequences were very conservative, whereas the theoretical values for low-high and low-high mixed stress sequences were in better agreement with the experimental fatigue life values.

CHAPTER VI

CONCLUSIONS

From the discussion of results it can be concluded that the predicted fatigue failure values using Kramer's cumulative fatigue damage equation for the low-high and low-high mixed stress sequences under completely reversed stress conditions, R=-1, are in complete agreement with the experimental values, while the theoretical values for high-low and high-low mixed stress sequences were very conservative as compared with those obtained experimentally.

For the low-high and low-high mixed stress sequences under stress ratio of R=-0.5, the cumulative fatigue damage values determined experimentally were mostly in the range of 0.80 - 0.96. From these results it can be concluded that the theoretical fatigue failure values were in close agreement with those obtained experimentally. For the high-low and high-low mixed stress sequences, the experimental values were in the range 1.35 - 2.5, from which it can be concluded that the theoretical fatigue failure values were very conservative.

The experimental values for the low-high and low-high mixed stress sequences under the stress ratio R=0 were in the range of 1.00 - 1.16. Even though the experimental values in the final stage were higher than the theoretical values, it can be concluded that cumulative fatigue damage predicted by Kramer's equation was in close agreement with the experimental values. The experimental values for

the high-low and high-low mixed stress sequences were in the range of 2.03 - 2.92 from which it can be concluded that the theoretical values were very conservative.

From the data for high-low and high-low mixed stress sequences under the three stress ratios R=-1, R=-0.5, and R=0, it can be concluded that cycling at a higher stress initially and then reducing the maximum stress applied in the subsequent stages increases the surface layer stress, thereby increasing the fatigue life.

A further important conclusion which can be drawn is that the accuracy for predicting the cumulative fatigue damage depends on the material constants P and δ. Therefore, the accuracy of S-N curves is very important for analyzing fatigue data using Kramer's equation.

CHAPTER VII

RECOMMENDATIONS

It is recommended that tests be continued to generate fatigue data on various other alloys of practical use. Also, the Kramer's equation for predicting cumulative fatigue damage be modified so as to predict the damage for high-low and high-low mixed stress sequences more realistically.

A P P E N D I C E S

APPENDIX A

FIGURES

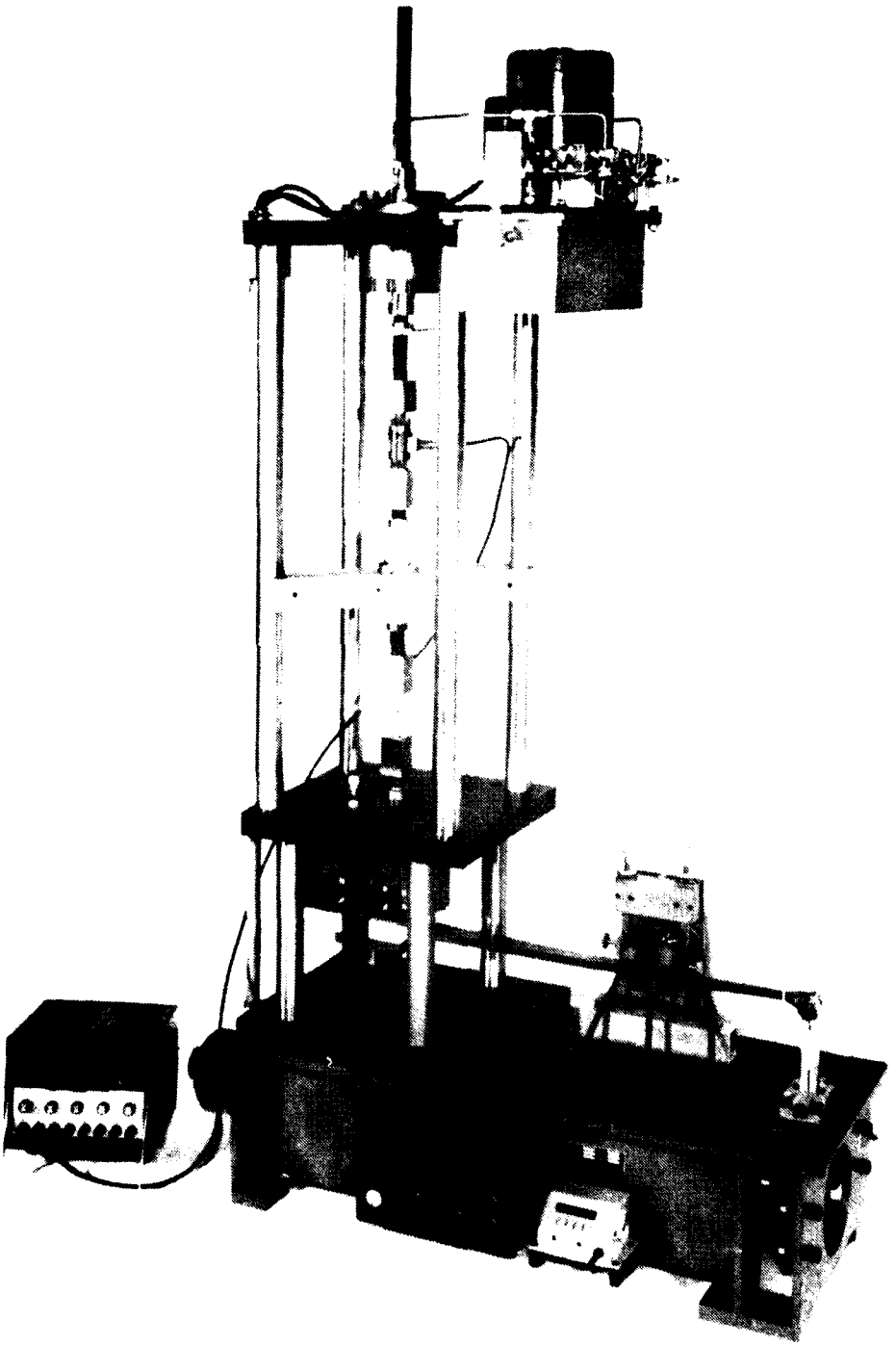

Fig. 1. Model DS 600 HLM Fatigue Machine.

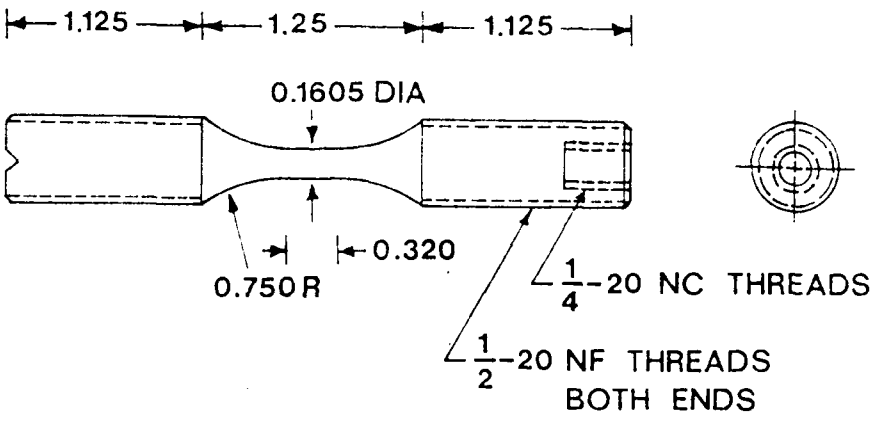

Fig. 2. Fatigue Specimen.

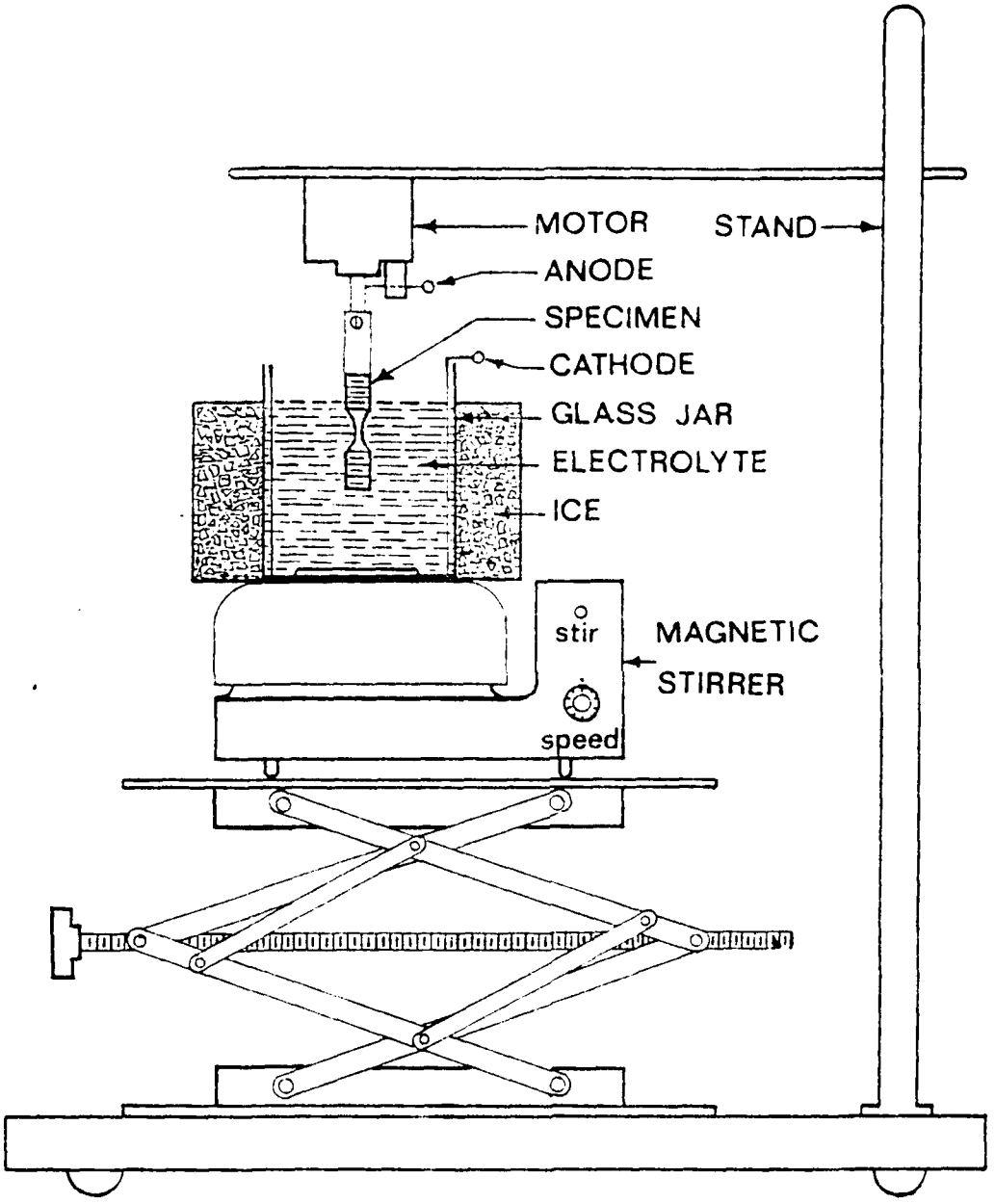

Fig. 3. Electropolishing Apparatus.

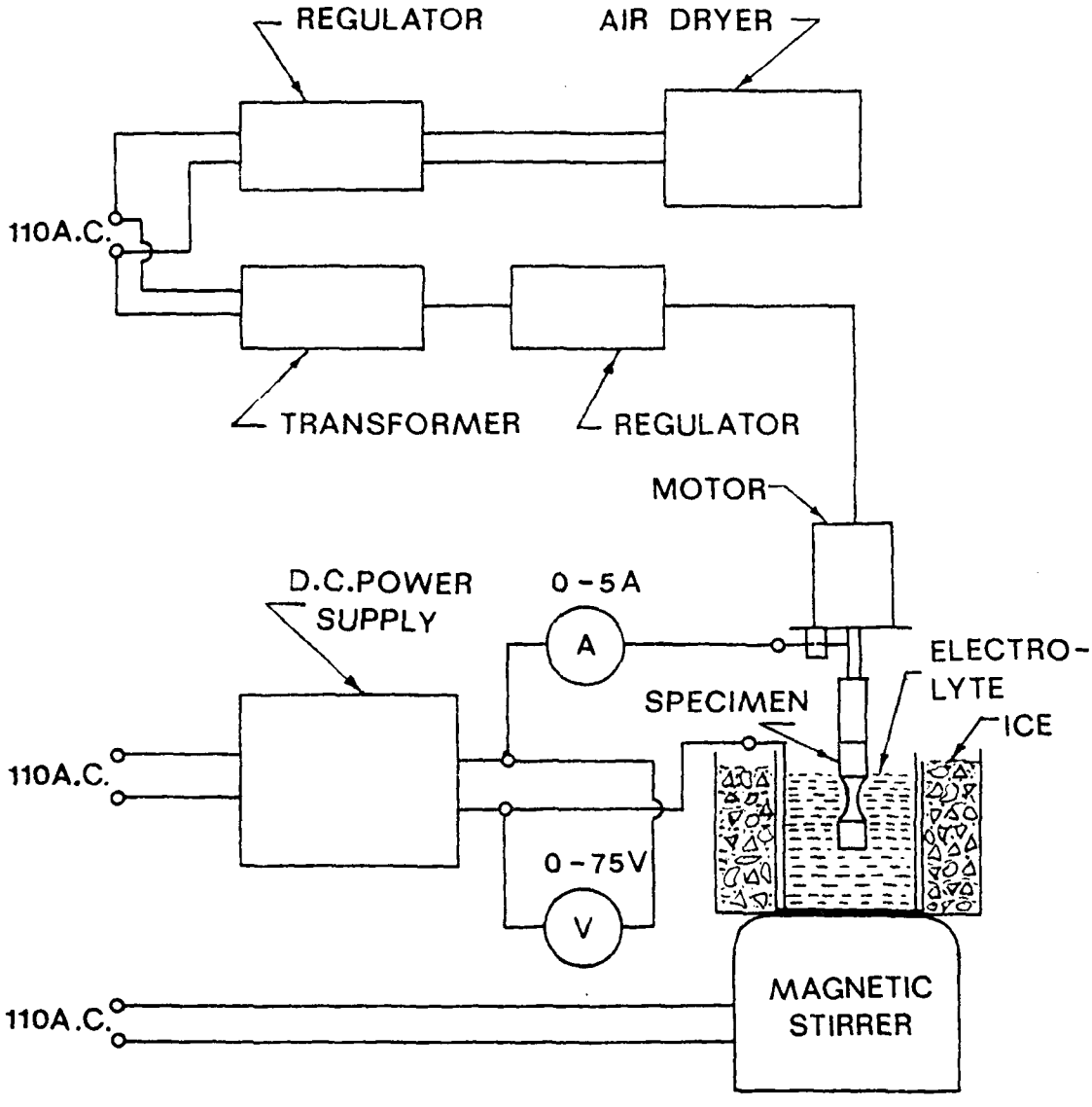

Fig. 4. Block Diagram for Electropolishing.

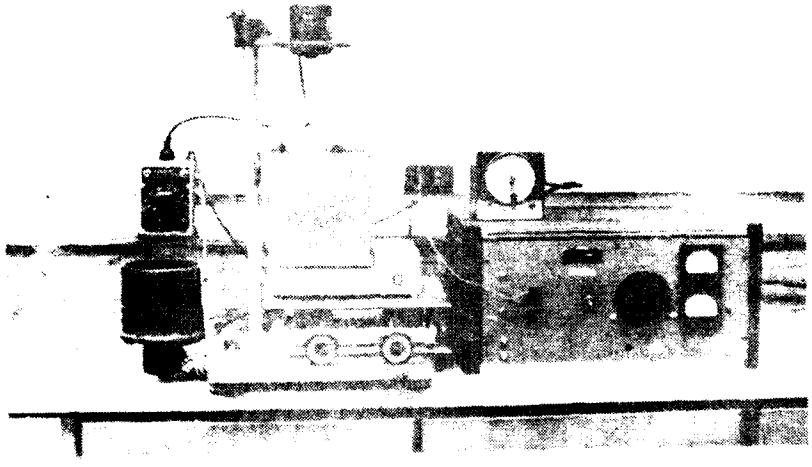

Fig. 5. Electropolishing System.

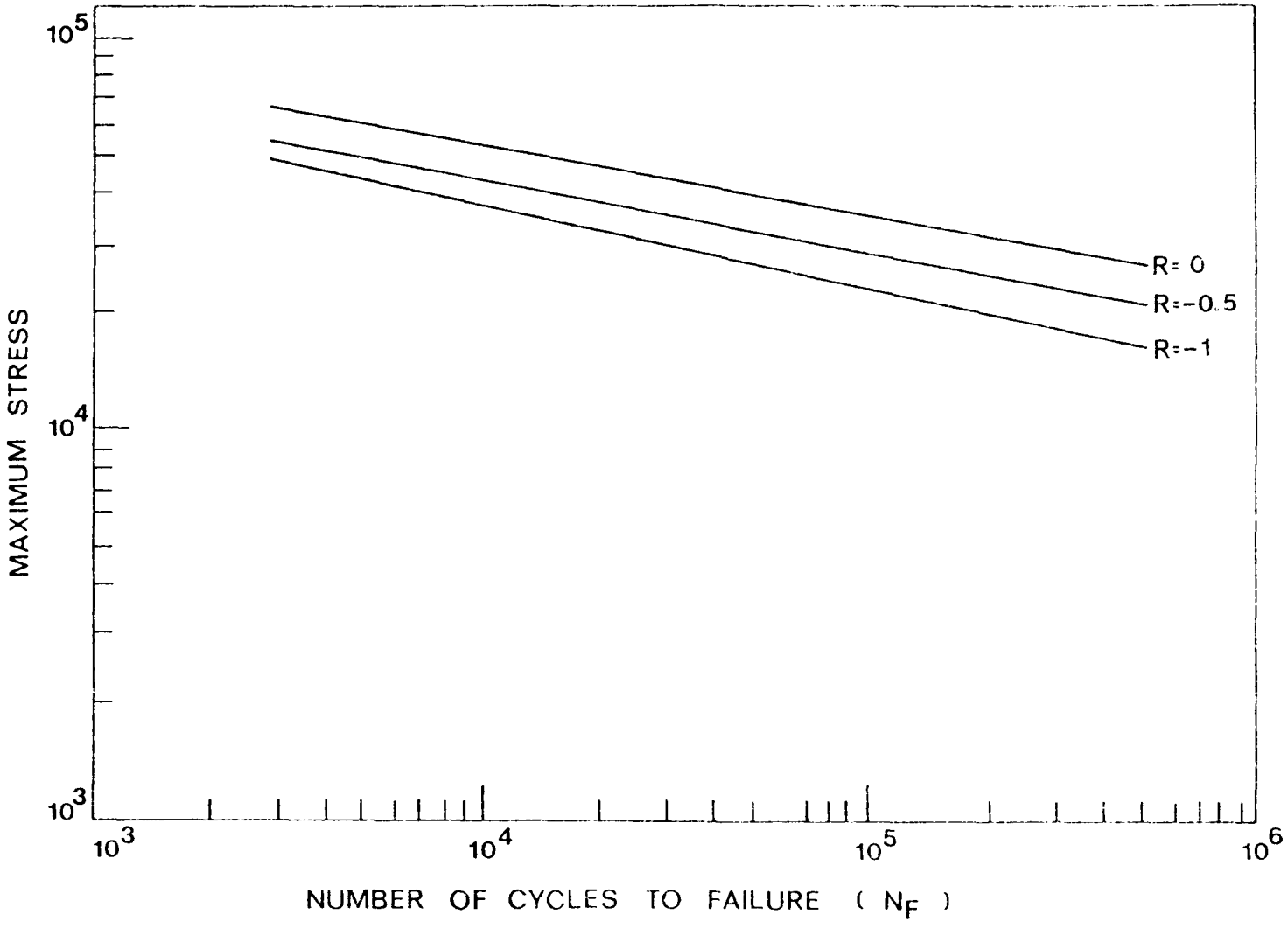

Fig. 6. S-N Diagrams for 2011-T3 Aluminum Alloy.

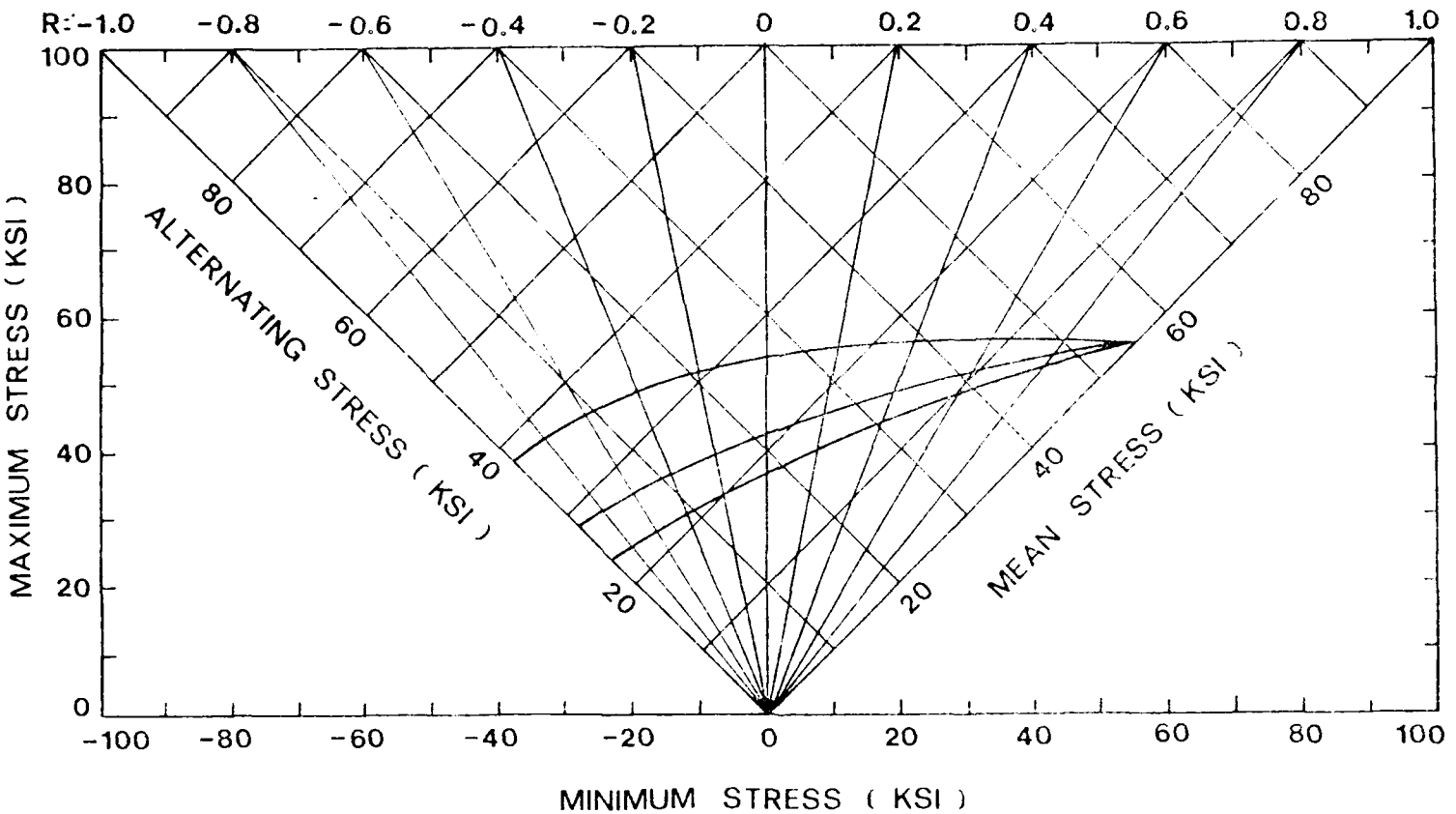

Fig. 7. Constant Fatigue Life Diagram for 2011-T3 Aluminum Alloy.

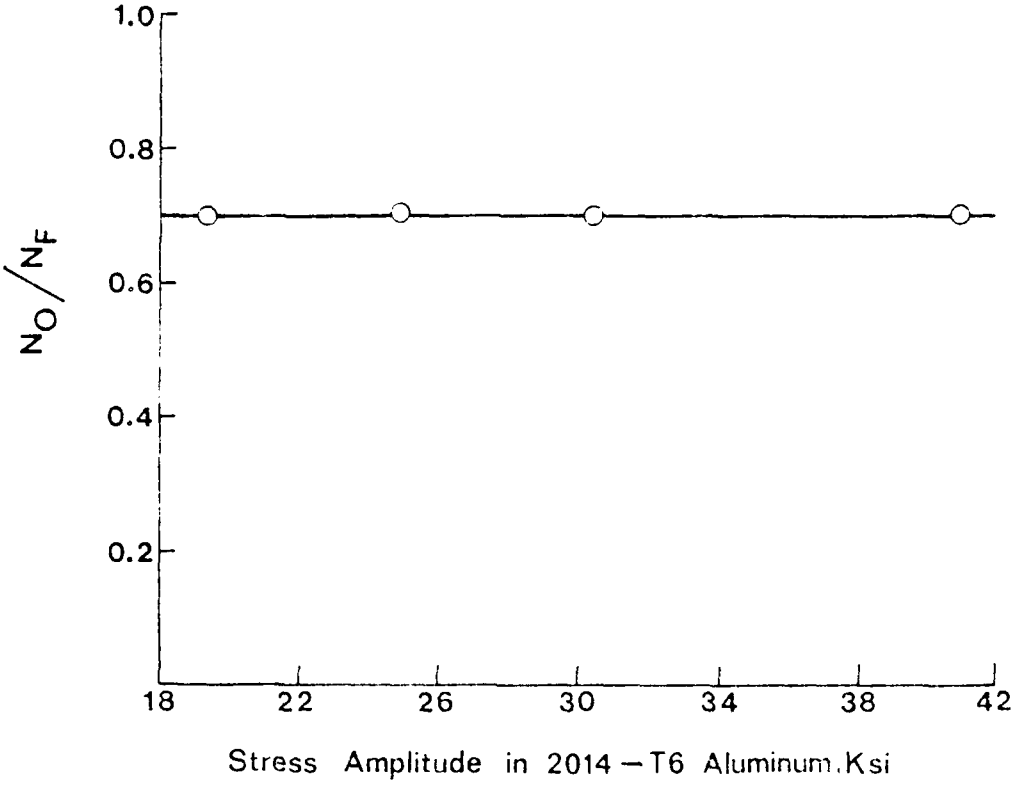

Fig. 8. N_O/N_F As A Function of Stress Amplitude.

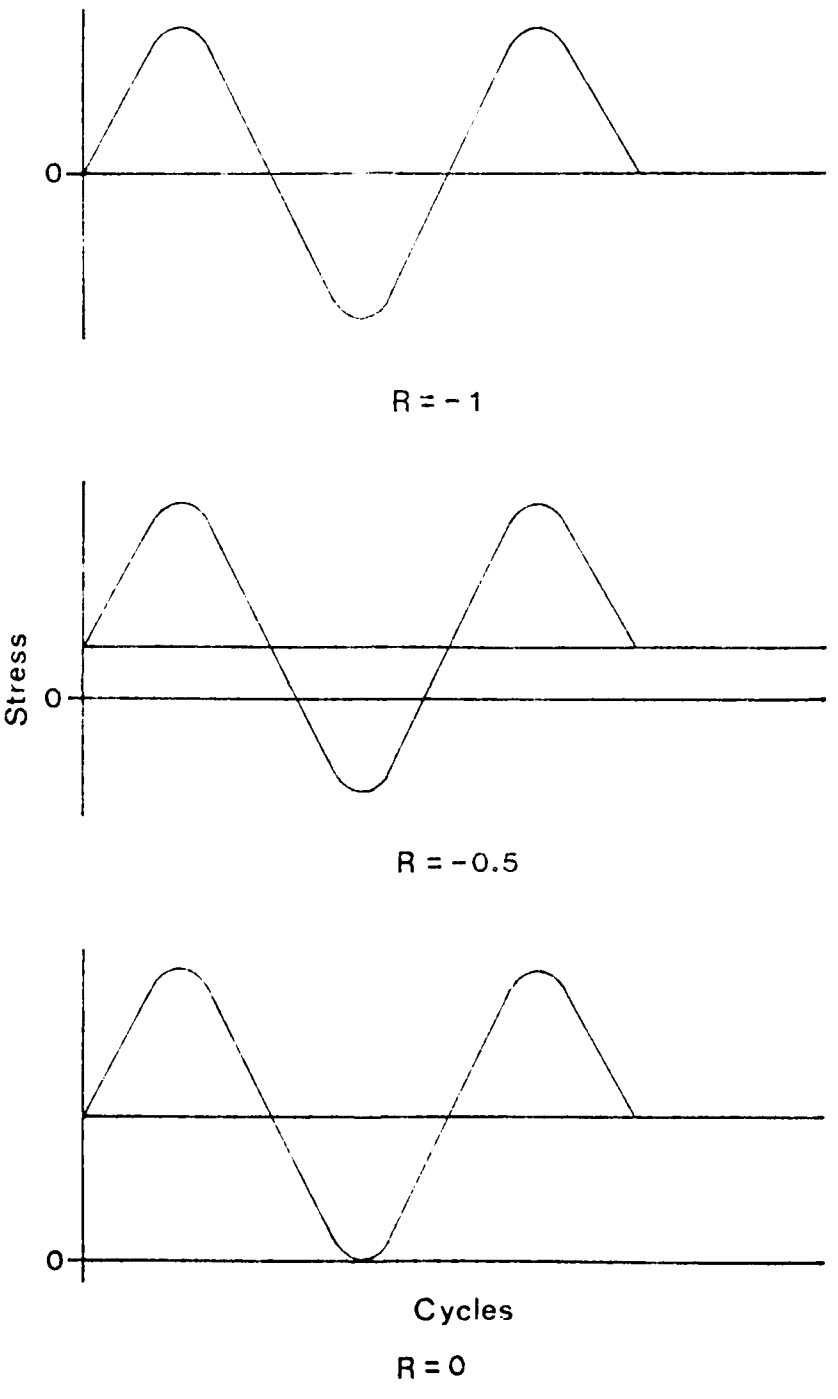

Fig. 9. Stress Ratios Vs Cycles.

APPENDIX B

T A B L E S

TABLE 1

EXPERIMENTAL DATA FOR S-N CURVE (R=-1)

No.	Max. Stress (PSI)	No. of Cycles to Failure (N)
1	42300	4100
2	36800	8000
3	34600	11400
4	32100	20500
5	30800	34700
6	28800	42600
7	26800	72600
8	23900	81600
9	22100	147000
10	19100	289000

TABLE 2

EXPERIMENTAL DATA FOR S-N CURVE (R=-$\frac{1}{3}$)

No.	Max. Stress (PSI)	No. of Cycles to Failure (N)
1	46000	6800
2	42800	12300
3	41100	15500
4	38400	25500
5	35800	28200
6	31800	59500
7	29400	76600
8	24900	211000

TABLE 3

EXPERIMENTAL DATA FOR S-N CURVE (R=0)

No.	Max. Stress (PSI)	No. of Cycles to Failure (N)
1	47700	17000
2	44300	57000
3	44300	26500
4	38300	72800
5	33800	101000
6	29800	270000
7	26900	340000
8	26900	640000

TABLE 4

CUMULATIVE FATIGUE DATA FOR LOW-HIGH STRESS SEQUENCE (R=-1)

S. No.		Stage 1 25000 PSI	Stage 2 30000 PSI	Stage 3 35000 PSI	*Stage 4 - 40000 PSI	
					Theoret-ical	Experi-mental
1	Numbers of Cycles	20000	8000	4000	2397	1300
2		20000	8000	4000	2397	2400
3		20000	8000	4000	2397	2200
4		20000	8000	4000	2397	2100
5		20000	8000	4000	2397	2100
6		20000	8000	4000	2397	2400
7		30000	10000	3000	1335	500
8		30000	10000	3000	1335	1100
9		30000	10000	3000	1335	1500
10		25000	10000	5000	996	700
11		25000	10000	5000	996	1200
12		25000	10000	5000	996	1000
		20000 PSI	25000 PSI	30000 PSI	35000 PSI	
13		35000	30000	15000	1890	1700
14		25000	30000	15000	1890	1500
15		35000	30000	15000	1890	1800
16		40000	28000	16000	1373	1200
17		40000	28000	16000	1373	1100
18		40000	28000	16000	1373	350

*Specimen is stressed till failure in the 4th stage.

TABLE 5

CUMULATIVE FATIGUE DATA FOR LOW-HIGH MIXED STRESS SEQUENCE (R=-1)

S. No.		Stage 1 25000 PSI	Stage 2 30000 PSI	Stage 3 35000 PSI	*Stage 4 - 40000 PSI	
					Theoret-ical	Experi-mental
1	Numbers of Cycles	20000	4000	8000	2689	2700
2		20000	4000	8000	2689	2400
3		20000	4000	8000	2689	3200
4		20000	4000	8000	2689	2800
5		20000	4000	8000	2689	2650
6		20000	4000	8000	2689	2800
7		30000	3000	10000	1161	1200
8		30000	3000	10000	1161	800
9		30000	3000	10000	1161	1200
10		25000	5000	11000	462	900
11		25000	5000	11000	462	600
12		25000	5000	11000	462	1050
		20000 PSI	30000 PSI	25000 PSI	35000 PSI	
13		35000	15000	25000	132	200
14		35000	15000	25000	132	700
15		35000	15000	25000	132	300
16		40000	16000	20000	1551	900
17		40000	16000	20000	1551	1300
18		40000	16000	20000	1551	1650

*Specimen is stressed till failure in the 4th stage.

TABLE 6

CUMULATIVE FATIGUE DATA FOR HIGH-LOW STRESS SEQUENCE (R=-1)

S. No.		Stage 1 40000 PSI	Stage 2 35000 PSI	Stage 3 30000 PSI	*Stage 4 - 25000 PSI	
					Theoret-ical	Experi-mental
1		1500	4000	8000	6923	50100
2		1500	4000	8000	6923	33700
3		1500	4000	8000	6923	44200
4		1500	4000	8000	6923	54900
5		1500	4000	8000	6923	52000
6		1500	4000	8000	6923	47000
				**Stage 3		*Stage 4 25000 PSI
				Theoret-ical	Experi-mental	
7	Cycles Applied	2500	6000	3720	15000	27000
8		2500	6000	3720	15000	24500
9		2500	6000	3720	15000	25300
10		3000	5000	4920	20000	20100
11		3000	5000	4026	20000	17600
12		3000	5000	4026	20000	19200
		35000 PSI	30000 PSI	25000 PSI		20000 PSI
13		5000	12000	4721	25000	39700
14		5000	12000	4721	25000	52200
15		5000	12000	4721	25000	46000
16		4000	15000	4996	30000	28500
17		4000	15000	4996	30000	13000
18		4000	15000	4996	30000	37900

*Specimen is stressed till failure in 4th stage.
**Theoretically failure should have occurred in the 3rd stage.

TABLE 7

CUMULATIVE FATIGUE DATA FOR HIGH-LOW MIXED STRESS SEQUENCE (R=-1)

S. No.		Stage 1 40000 PSI	Stage 2 30000 PSI	Stage 3 35000 PSI	*Stage 4 - 25000 PSI	
					Theoret-ical	Experi-mental
1		1500	8000	4000	10959	73600
2		1500	8000	4000	10959	71200
3		1500	8000	4000	10959	80000
4		1500	8000	4000	10959	68000
5		1500	8000	4000	10959	72000
6		1500	8000	4000	10959	66900
				**Stage 3 - 35000 PSI		Stage 4 25000 PSI
				Theoret-ical	Experi-mental	
7	Cycles Applied	3500	9000	516	5000	53000
8		3500	9000	516	5000	47400
9		3500	9000	516	5000	55900
10		3000	11000	381	7000	45200
11		3000	11000	381	7000	38500
12		3000	11000	381	7000	41100
		35000 PSI	25116 PSI	30090 PSI		20142 PSI
13		5000	15000	8680	30000	29000
14		5000	15000	8680	30000	34100
15		5000	15000	8680	30000	37300
16		4000	18000	19417	35000	22900
17		4000	18000	19417	35000	26000
18		4000	18000	19417	35000	23400

*Specimen is stressed till failure in 4th stage.
**Theoretically failure should have occurred in the third stage.

TABLE 8

CUMULATIVE FATIGUE DATA FOR HIGH-LOW STRESS SEQUENCE (R=-0.5)

S. No.		Stage 1 40000 PSI	Stage 2 35000 PSI	Stage 3 30000 PSI		*Stage 4 - 25000 PSI	
						Theoret-ical	Experi-mental
1	Cycles Applied	4000	3000	30000		6950	56700
2		4000	8000	30000		6950	58700
				**Stage 3 - 30000 PSI		*Stage 4 25000 PSI	
				Theoret-ical	Experi-mental		
3		5000	7000	31740	35000	37800	
4		5000	7000	31740	35000	60100	

TABLE 9

CUMULATIVE FATIGUE DATA FOR HIGH-LOW (MIXED) STRESS SEQUENCE (R=-0.5)

S. No.		Stage 1 40000 PSI	Stage 2 30000 PSI	Stage 3 35000 PSI		*Stage 4 - 25000 PSI	
						Theoret-ical	Experi-mental
1	Cycles Applied	4000	30000	8000		16695	64900
2		4000	30000	8000		16695	65200
				**Stage 3 - 35000 PSI		Stage 4 25000 PSI	
				Theoret-ical	Experi-mental		
3		5000	35000	3530	7000	41500	
4		5000	35000	3530	7000	61600	

*Specimen is stressed til failure in the 4th stage.

**Theoretically failure should have occurred in the 3rd stage.

TABLE 10

CUMULATIVE FATIGUE DATA FOR LOW-HIGH STRESS SEQUENCE (R=-0.5)

No.		Stage 1 25000 PSI	Stage 2 30000 PSI	Stage 3 35000 PSI	*Stage 4 - 40000 PSI	
					Theoret-ical	Experi-mental
1	Cycles Applied	60000	30000	8000	6104	2300
				**Stage 3 - 35000 PSI		
				Theoret-ical	Experi-mental	
2		60000	30000	22392	6500	
3		60000	30000	22392	7900	
4		50000	35000	22918	7100	
5		50000	35000	22918	7700	

TABLE 11

CUMULATIVE FATIGUE DATA FOR LOW-HIGH (MIXED) STRESS SEQUENCE (R=-0.5)

No.		Stage 1 25000 PSI	Stage 2 35000 PSI	**Stage 3 - 30000 PSI	
				Theoretical	Experimental
1	Cycles Applied	60000	8000	48644	27000
2		60000	8000	48644	7500
3		6000	8000	48644	22400
4		50000	9000	48335	33700
5		50000	9000	48335	28200

*Specimen is stressed till failure in 4th stage.
**Specimen is not stressed till failure in this stage, even though failure took place.

TABLE 12

CUMULATIVE FATIGUE DATA FOR HIGH-LOW STRESS SEQUENCE (R=0)

No.		Stage 1 40000 PSI	Stage 2 35000 PSI	Stage 3 30000 PSI	*Stage 4 - 25000 PSI	
					Theoret-ical	Experi-mental
1	Cycles Applied	12000	25000	50000	144610	383200
2		12000	25000	50000	144610	397900
3		20000	30000	40000	27893	159300
4		20000	30000	40000	27893	207000

TABLE 13

CUMULATIVE FATIGUE DATA FOR HIGH-LOW MIXED STRESS SEQUENCE (R=0)

No.		Stage 1 40000 PSI	Stage 2 30000 PSI	Stage 3 35000 PSI	*Stage 4 - 25000 PSI	
					Theoret-ical	Experi-mental
1	Cycles Applied	20000	50000	25000	42564	306300
2		20000	50000	25000	42564	284000
3		25000	40000	20000	24777	291100
4		25000	40000	20000	24777	276100

*Specimen is stressed till failure in the 4th stage.

TABLE 14

CUMULATIVE FATIGUE DATA FOR LOW-HIGH STRESS SEQUENCE (R=0)

No.		Stage 1 25000 PSI	Stage 2 20000 PSI	Stage 3 35000 PSI	*Stage 4 - 40000 PSI	
					Theoret-ical	Experi-mental
1	Cycles Applied	150000	40000	20000	31848	52300
2		150000	40000	20000	31848	61700
3		200000	45000	15000	28812	49900
4		200000	45000	15000	28812	45800

TABLE 15

CUMULATIVE FATIGUE DATA FOR LOW-HIGH MIXED STRESS SEQUENCE (R=0)

No.		Stage 1 25000 PSI	Stage 2 35000 PSI	Stage 3 30000 PSI	*Stage 4 - 40000 PSI	
					Theoret-ical	Experi-mental
1	Cycles Applied	200000	25000	45000	29531	78000
2		200000	25000	45000	29531	67100
3		150000	30000	40000	31021	67900
4		150000	30000	40000	31021	69500

*Specimen is stressed till failure in the 4th stage.

TABLE 19

CUMULATIVE FATIGUE DAMAGE FOR LOW-HIGH STRESS SEQUENCE (R=-1)

S. No.	D_F Kramer	D_F Miner	N_F Theoretical	N_F Experimental	$\frac{N_F(\text{Exp.})}{N_F(\text{Theo.})}$
1	0.881	1.011	34397	33300	0.968
2	0.994	1.187	34397	34400	1.000
3	0.974	1.124	34397	34200	0.994
4	0.963	1.111	34397	34100	0.991
5	0.963	1.111	34397	34100	0.991
6	0.994	1.187	34397	34400	1.000
7	0.911	1.056	44335	43500	0.982
8	0.975	1.133	44335	44100	0.995
9	1.018	1.184	44335	44500	1.004
10	0.971	1.145	40996	40700	0.993
11	1.020	1.208	40996	41200	1.005
12	1.000	1.183	40996	41000	1.000
13	1.006	1.267	81890	81700	0.998
14	0.997	1.253	81890	81500	0.995
15	1.011	1.274	81890	81800	0.999
16	1.006	1.263	85373	85200	0.998
17	1.004	1.257	85373	85100	0.997
18	0.992	1.239	85373	84850	0.994

D_F = Cumulative fatigue damage = $f_1 + f_2 + f_3 + f_4$.

N_F = Total number of cycles at failure.

N_F (Theoretical) = Total number of cycles at failure using Kramer's equation (Equation 2).

TABLE 1

CUMULATIVE FATIGUE DAMAGE FOR LOW-HIGH MIXED STRESS SEQUENCE (R=-1)

S. No.	D_F Kramer	D_F Miner	N_F Theoretical	N_F Experimental	$\frac{N_F(Exp.)}{N_F(Theo.)}$
1	1.002	1.167	34639	34700	1.002
2	0.975	1.144	34659	34400	0.992
3	1.044	1.230	34659	35200	1.015
4	1.011	1.189	34659	34800	1.003
5	0.997	1.180	34659	34650	0.999
6	1.010	1.199	34659	34800	1.004
7	1.006	1.146	44161	44200	1.001
8	0.971	1.096	44161	43600	0.987
9	1.011	1.159	44161	44300	1.003
10	1.032	1.200	41462	41900	1.010
11	1.010	1.165	41462	41900	1.008
12	1.045	1.222	41462	42050	1.014
13	1.003	1.089	75132	75200	1.001
14	1.021	1.123	75132	75700	1.008
15	1.006	1.096	75132	75300	1.002
16	0.985	1.134	77551	76900	0.992
17	1.003	1.151	77551	77300	0.997
18	1.017	1.175	77551	77650	1.001

D_F = Cumulative fatigue damage = $f_1 + f_2 + f_3 + f_4$.

N_F (Theoretical) = Total number of cycles at failure using Kramer's equation (Equation 2).

N_F = Total number of cycles at failure.

TABLE 15

CUMULATIVE FATIGUE DAMAGE FOR HIGH-LOW STRESS SEQUENCE (R=-1)

S. No.	D_F Kramer	D_F Miner	N_F Theoretical	N_F Experimental	$\frac{N_F(Exp.)}{N_F(Theo.)}$
1	1.960	1.501	20423	63600	3.114
2	1.596	1.252	20423	47200	2.371
3	1.829	1.411	20423	57700	2.825
4	2.067	1.573	20423	68400	3.349
5	2.003	1.529	20423	65500	3.207
6	1.891	1.454	20423	60500	2.962
7	2.716	1.654	12200	50500	4.133
8	2.625	1.621	12200	48300	3.953
9	2.646	1.629	12200	48800	3.994
10	2.859	1.717	12026	48100	4.000
11	2.729	1.679	12026	45600	3.792
12	2.812	1.703	12026	47200	3.925
13	2.171	1.360	21721	81700	3.761
14	2.370	1.430	21721	94200	4.337
15	2.271	1.395	21721	88000	4.051
16	2.429	1.439	23996	77500	3.230
17	2.487	1.428	23996	80000	3.334
18	2.647	1.462	23996	86900	3.621

D_F = Cumulative fatigue damage = $f_1 + f_2 + f_3 + f_4$.

N_F = Total number of cycles at failure.

N_F (Theoretical) = Total number of cycles at failure using Kramer's equation (Equation 2).

TABLE 19

CUMULATIVE FATIGUE DAMAGE FOR HIGH-LOW MIXED STRESS SEQUENCE (R=-1)

S. No.	D_F Kramer	D_F Miner	N_F Theoretical	N_F Experimental	$\frac{N_F(\text{Exp.})}{N_F(\text{Theo.})}$
1	2.315	1.857	24459	87100	3.561
2	2.264	1.821	24459	84700	3.463
3	2.449	1.954	24459	104459	4.271
4	2.197	1.772	24459	81500	3.332
5	2.281	1.833	24459	85500	3.496
6	2.174	1.755	24459	80400	3.287
7	2.566	1.898	13016	70300	5.416
8	2.431	1.813	13016	64900	4.986
9	2.636	1.942	13016	73400	5.639
10	2.632	1.922	14381	66200	4.603
11	2.449	1.821	14381	59500	4.137
12	2.520	1.860	14381	62100	4.318
13	2.447	1.771	28680	79000	2.755
14	2.586	1.799	28680	84100	2.932
15	2.673	1.817	28680	87300	3.044
16	2.549	1.587	32417	79900	2.465
17	2.662	1.904	32417	83000	2.560
18	2.568	1.890	32417	80400	2.480

D_F = Cumulative fatigue damage = $f_1 + f_2 + f_3 + f_4$.

N_F = Total number of cycles at failure.

N_F (Theoretical) = Total number of cycles at failure using Kramer's equation (Equation 2).

TABLE 20

CUMULATIVE FATIGUE DAMAGE FOR HIGH-LOW STRESS SEQUENCE (R=-0.5)

S. No.	D_F Kramer	D_F Miner	N_F Theoretical	N_F Experimental	$\frac{N_F(Exp.)}{N_F(Theo.)}$
1	1.402	1.063	48950	100700	2.057
2	1.132	0.905	48950	66000	1.348
3	1.370	1.056	43740	84800	1.939
4	1.559	1.157	43740	107100	2.449

TABLE 21

CUMULATIVE FATIGUE DAMAGE FOR HIGH-LOW MIXED STRESS SEQUENCE (R=-0.5)

S. No.	D_F Kramer	D_F Miner	N_F Theoretical	N_F Experimental	$\frac{N_F(Exp.)}{N_F(Theo.)}$
1	1.404	1.182	58695	12690	2.162
2	1.424	1.236	58695	13020	2.218
3	1.311	1.072	43530	38500	2.033
4	1.426	1.164	43530	108600	2.495

TABLE 22

CUMULATIVE FATIGUE DAMAGE FOR LOW-HIGH STRESS SEQUENCE (R=-0.5)

S. No.	D_F Kramer	D_F Miner	N_F Theoretical	N_F Experimental	$\frac{N_F(Exp.)}{N_F(Theo.)}$
1	0.[illegible]	0.[illegible]	104104	100[illegible]	[illegible]
2	0.[illegible]	0.799	112392	96500	0.859
3	0.703	0.837	112392	97900	0.871
4	0.[illegible]	0.828	107915	92100	0.853
5	0.704	0.845	107915	91700	0.850

TABLE 23

CUMULATIVE FATIGUE DAMAGE FOR LOW-HIGH MIXED STRESS SEQUENCE (R=-0.5)

S. No.	D_F Kramer	D_F Miner	N_F Theoretical	N_F Experimental	$\frac{N_F(Exp.)}{N_F(Theo.)}$
1	0.737	0.806	116644	95000	0.814
2	0.499	0.581	116644	75500	0.647
3	0.681	0.752	116644	90400	0.775
4	0.817	0.866	107335	92700	0.863
5	0.748	0.802	107335	87200	0.812

TABLE 24

CUMULATIVE FATIGUE DAMAGE FOR HIGH-LOW STRESS SEQUENCE (R=0)

S. No.	D_F Kramer	D_F Miner	N_F Theoretical	N_F Experimental	$\frac{N_F(Exp.)}{N_F(Theo.)}$
1	1.444	1.186	231610	470200	2.030
2.	1.471	1.206	231610	484900	2.094
3	1.245	1.031	117893	249300	2.115
4	1.339	1.096	117893	297000	2.519

TABLE 25

CUMULATIVE FATIGUE DAMAGE FOR HIGH-LOW MIXED STRESS SEQUENCE (R=0)

S. No.	D_F Kramer	D_F Miner	N_F Theoretical	N_F Experimental	$\frac{N_F(Exp.)}{N_F(Theo.)}$
1	1.487	1.231	137564	401300	2.917
2	1.445	1.200	137564	379000	2.755
3	1.495	1.188	109777	376100	3.426
4	1.492	1.169	109777	361100	3.289

TABLE 26

CUMULATIVE FATIGUE DAMAGE FOR LOW-HIGH STRESS SEQUENCE (R=0)

S. No.	D_F Kramer	D_F Miner	N_F Theoretical	N_F Experimental	$\frac{N_F(Exp.)}{N_F(Theo.)}$
1	1.333	1.506	241848	262300	1.084
2	1.486	1.681	241848	271700	1.123
3	1.354	1.483	288812	309900	1.070
4	1.286	1.407	288812	305900	1.059

TABLE 27

CUMULATIVE FATIGUE DAMAGE FOR LOW-HIGH MIXED STRESS SEQUENCE (R=0)

S. No.	D_F Kramer	D_F Miner	N_F Theoretical	N_F Experimental	$\frac{N_F(Exp.)}{N_F(Theo.)}$
1	1.686	2.114	299531	348000	1.162
2	1.532	1.912	299531	337100	1.125
3	1.536	1.887	251020	287900	1.147
4	1.559	1.916	251020	289500	1.153

APPENDIX C

NOMENCLATURE

D_F = Cumulative fatigue damage

D_F (Kramer) = Cumulative fatigue damage using Kramer's equation (Equation 2)

D_F (Miner) = Cumulative fatigue damage using Miner's equation

$f_1 f_2 \ldots$ = Fatigue damage prehistories

m = Slope of the S-N curve which is in the form $\log Y = m.\log X + \log C$

$N_1, N_2 \ldots$ = Number of cycles applied at each stress

N_F (Theo) = Total number or cycles at failure, obtained theoretically using Kramer's equation (Equation 2)

N_F (Exp.) = Total number of cycles to failure obtained experimentally

p = Material constant = $-\frac{1}{m}$

R = Stress ratio = $\frac{\text{Minimum Stress}}{\text{Maximum Stress}}$

σ_{mean} = Mean Stress = $\frac{\text{Maximum Stress} + \text{Minimum Stress}}{2}$

$\sigma_1, \sigma_2 \ldots$ = Maximum stress applied at each stage of testing

σ_s^* = Critical surface layer stress

α = Material constant

β = Material constant = $(\log^{-1} C)^p$

APPENDIX D

KRAMER'S WORK

I. R. Kramer conducted experiments on 2014-T6 aluminum alloy and showed that while materials are subjected to fatigue cycles, the work hardening of surface layer takes place and consequently the proportional limit for the material is increased with increased number of cycles. He defined this increase in proportional limit as the surface layer strength (σ_s). He further stated that when this surface layer stress reached a critical value (σ_s^*) the failure producing crack propagated. He showed that σ_s^* is independent of the stress magnitude. He also measure the ratio of N_o/N_F to determine whether it varied with stress amplitude, as shown in Figure 8. He found that over the stress range employed, this ratio was independent of the stress amplitude.

N_o = Number of cycles to initiate the propagating crack

N_F = Number of cycles to failure

$\frac{N_o}{N_F}$ = A constant = 0.7 for aluminum

S = Slope = $d\sigma_s/dN$

σ_s = SN or

σ_s^* = SN_o

$D = \frac{\sigma_s}{\sigma_s^*}$ = Fatigue damage to initiate a propagating crack, and the crack will be initiated when $\varepsilon\sigma_{si}/\sigma_s^* = 1$, or $\varepsilon \frac{N_i}{N_o} = 1$

The incremental rate of change of surface stress σ_s at the first stress level is given by $S_I = \alpha\sigma_1^P$. After N_1 cycles, the maximum stress is increased to σ_2 and the incremental rate of change of surface stress at this second level will be modified as

$$S_{II} = \left(\frac{S_1}{S_1}\right)^{f_1} \alpha\sigma_2^P$$

$$S_{II} = \left(\frac{\sigma_1}{\sigma_2}\right)^{Pf_1} \alpha\sigma_2^P.$$

Similarly, at the third level, $S_{III} = \left(\frac{S_{II}}{S_3}\right)^{f_2} \alpha\sigma_3^P$.

Substituting for S_{II} gives $S_{III} = \left(\frac{\sigma_1}{\sigma_2}\right)^{Pf_1} \frac{\alpha\sigma_2^{Pf_2}}{\alpha\sigma_3^P} \alpha\sigma_3^P$

$$= \left(\frac{\sigma_1}{\sigma_2}\right)^{Pf_1f_2} \left(\frac{\sigma_2}{\sigma_3}\right)^{Pf_2} \alpha\sigma_3^P$$

and so on. Failure occurs when $N_1S_1 + N_2S_2\,(S_1/S_2)^{f_1} + \ldots = \sigma_s^*$, where the subscripts denote the consecutive changes in the alternating stress amplitude. From the relation between $d\sigma_s/d_N$ and α he had shown that $S = \alpha\sigma^P$. So, substituting $S = \alpha\sigma^P$ in the above equation, he obtained

$$\sigma_1^P N_1 + \sigma_2^P N_2 \left(\frac{\sigma_1}{\sigma_2}\right)^{Pf_1} + \sigma_3^P N_3 \left(\frac{\sigma_2}{\sigma_3}\right)^{Pf_2} \left(\frac{\sigma_1}{\sigma_2}\right)^{Pf_2f_1} + \ldots = \frac{\sigma_s^*}{\alpha} = \beta$$

Dividing throughout by β he obtained

$$\frac{\sigma_1^P N_1}{\beta} + \frac{\sigma_2^P N_2}{\beta}\left(\frac{\sigma_1}{\sigma_2}\right)^{Pf_1} + \frac{\sigma_3^P N_3}{\beta}\left(\frac{\sigma_2}{\sigma_3}\right)^{Pf_2}\left(\frac{\sigma_1}{\sigma_2}\right)^{Pf_2f_1} + \ldots = 1.$$

APPENDIX E

SPECIMEN PREPARATION

1. The specimen is to be machined as per the specifications in the drawing.
2. The tool marks on the surface where the polishing is to be done should be cleaned using the finest grade of silicon carbide sandpaper.
3. The specimen should be heat-treated and tempered back to the pre-machining metalurgical conditions of the metal used (2011-T3).
4. The surface to be polished should be washed with methanol and dried.
5. The specimen should be examined using a microscope for circumferential scratches or tool marks on the surface to be polished. If any scratches are found they should be removed.
6. Attach the specimen to the shaft of the stirrer.
7. The electrolyte should be prepared by using 59% methanol, 35% butyl cellosolve, and 6% perchloric acid.
8. The electrolyte temperature should be kept at 15°C.
9. Adjust the speed of the magnetic stirrer at 4.5.
10. Start the motor holding the specimen and the magnetic stirrer. Care should be taken to see that the specimen rotates in the direction opposite to that of the magnetic stirrer.
11. Immerse the specimen in the electrolyte, by raising the platform. until the surface which is to be polished is completely immersed. Allow the specimen to cool in the electrolyte for 20 seconds.
12. Set the voltage at 15-20 volts (1.2 - 1.5 amps) and adjust the timer for 2 minutes. Turn on the power to start the polishing.
13. At the end of 2 minutes, turn off the power and lower the platform. Stop the motor and remove the specimen.
14. Rinse the specimen with hot water and methanol and dry it in the air dryer.

15. After drying, the specimen should be carefully examined under the microscope at 10 X magnification to see if all the surface irregularities are removed. If any irregularities are still observed, the whole process should be repeated again starting from step 5.

16. If no irregularities are found, the specimen should be carefully wrapped in cotton and stored in the desicator.

LITERATURE CITED

1. Miner, M. A. 1945. Cumulative damage in fatigue. J. Applied Mechanics, 12:159-164.

2. Grover, H. J. 1960. An observation concerning the cycle ratio in cumulative damage. Symposium on Fatigue of Aircraft Structures, American Society for Testing Materials. Special Technical Publication No. 274, p. 120.

3. Marco, S. M. and W. L. Starkey. 1954. A concept of fatigue damage. Trans. Am. Soc. Mech. Eng., 76:627-632.

4. Shenley, F. R. 1952. "A Theory of Fatigue Based on Unbonding During Reversed Slip," The Rand Corporation, p. 356.

5. Corten, H. T. and T. J. Dolan. 1956. Cumulative Fatigue Damage. Proceedings of International Conference on Fatigue of Metals, Institution of Mechanical Engineers and American Society of Mechanical Engineers, pp. 235-246.

6. Freudenthal, A. M. and R. A. Heller. 1959. On stress interaction in fatigue and a cumulative damage rule. J. Aerospace Engineering, 28(7):431-442.

7. Kramer, I. R. 1976. A mechanism of fatigue failure. Metallurgical Transactions, 5:1735-1742.

8. Kramer, I. R. 1976. Prediction of Fatigue Damage. Proceedings of Second International Conference of Mechanical Behavior of Materials, pp. 812-816.

ACKNOWLEDGEMENTS

The authors wish to express their appreciation to the Department of Mechanical Engineering, Tuskegee Institute, Tuskegee Institute, Alabama, for providing assistance and facilities for this study.

Gratitude is also expressed to Dr. S. Z. Jarkowski and Dr. I. R. Kramer for their consultations throughout this research.

Finally, the authors express their thanks to the Department of the Navy, Naval Air Systems Command, Washington, DC, for providing financial support for this research through their grant No. N00019-80-C-0364.

Unclassified
SECURITY CLASSIFICATION OF THIS PAGE (When Data Entered)

REPORT DOCUMENTATION PAGE

READ INSTRUCTIONS BEFORE COMPLETING FORM

1 REPORT NUMBER: TI-NAVY-3	2 GOVT ACCESSION NO: AD A116 513
3 RECIPIENT'S CATALOG NUMBER:	
4 TITLE and Subtitle: A Study of Cumulative Fatigue Damage in 2011-T3 Aluminum Alloy	5 TYPE OF REPORT & PERIOD COVERED: Technical
6 PERFORMING ORG. REPORT NUMBER: TI-NAVY-3	
7 AUTHOR(s): Shaik Jeelani Purandar A. Reddy	8 CONTRACT OR GRANT NUMBER(s): N00019-80-C-0564
9 PERFORMING ORGANIZATION NAME AND ADDRESS: Tuskegee Institute Tuskegee, Alabama 36088	10 PROGRAM ELEMENT, PROJECT, TASK AREA & WORK UNIT NUMBERS:
11 CONTROLLING OFFICE NAME AND ADDRESS: Department of the Navy Naval Air Systems Command Washington, D.C.	12 REPORT DATE: August 1981 13 NUMBER OF PAGES: 67
14 MONITORING AGENCY NAME & ADDRESS (if different from Controlling Office)	15 SECURITY CLASS. (of this report): Unclassified 15a DECLASSIFICATION/DOWNGRADING SCHEDULE:

16 DISTRIBUTION STATEMENT (of this Report): Approved for Public Release; Distribution Unlimited

17 DISTRIBUTION STATEMENT (of the abstract entered in Block 20, if different from Report)

18 SUPPLEMENTARY NOTES

19 KEY WORDS (Continue on reverse side if necessary and identify by block number): Fatigue, Life, Endurance Limit, Cycles, Stress

20 ABSTRACT (Continue on reverse side if necessary and identify by block number)

This report describes the experimental facility developed at Tuskegee Institute, Tuskegee, Alabama, to study the effect of cumulative fatigue damage in selected materials. The equipment procured consists of direct tension-compression fatigue testing machines Model DS-600 HLM and DS-6000 HLM instrumented to conduct fatigue tests on Aluminum, steel and super alloys

DD FORM 1 JAN 73 1473 EDITION OF 1 NOV 65 IS OBSOLETE

Unclassified
SECURITY CLASSIFICATION OF THIS PAGE (When Data Entered)

Unclassified

SECURITY CLASSIFICATION OF THIS PAGE(When Data Entered)

20.

under various stress sequences.

Specimen profiler, heat treatment furnace and electro-polishing apparatus were purchased and/or developed for specimen preparation.

Experimental data were generated using 2011-T3 aluminum alloy specimens under stress ratios R=-1, R=-0.5, and R=0, for low-high, low-high mixed, and high-low mixed stress sequences.

Analysis of the data has indicated that the predicted cumulative fatigue damage and fatigue life are in close agreement for low-high and low-high mixed stress sequences under all stress ratios as compared with those obtained experimentally, whereas the theoretical values for high-low and high-low mixed stress sequences under all stress ratios were more conservative than those obtained experimentally.